Available online at www.sciencedirect.com

jmr&t Journal of Materials Research and Technology

journal homepage: www.elsevier.com/locate/jmrt

Use of calcium carbonate nanoparticles in production of nano-engineered foamed concrete

Md Azree Othuman Mydin [a,**], P. Jagadesh [b], Alireza Bahrami [c,*], Anmar Dulaimi [d,e], Yasin Onuralp Özkılıç [f,***], Mohd Mustafa Al Bakri Abdullah [g,h], Ramadhansyah Putra Jaya [i]

[a] School of Housing, Building and Planning, Universiti Sains Malaysia, Penang 11800, Malaysia
[b] Department of Civil Engineering, Coimbatore Institute of Technology, Tamil Nadu, 638 056, India
[c] Department of Building Engineering, Energy Systems and Sustainability Science, Faculty of Engineering and Sustainable Development, University of Gävle, 801 76 Gävle, Sweden
[d] College of Engineering, University of Warith Al-Anbiyaa, Karbala, Iraq
[e] School of Civil Engineering and Built Environment, Liverpool John Moores University, Liverpool L3 2ET, UK
[f] Department of Civil Engineering, Faculty of Engineering, Necmettin Erbakan University, Konya, Turkey
[g] Centre of Excellence Geopolymer and Green Technology, Universiti Malaysia Perlis, Arau 01000, Perlis, Malaysia
[h] Faculty of Chemical Engineering and Technology, Universiti Malaysia Perlis, Arau 01000, Perlis, Malaysia
[i] Faculty of Civil Engineering Technology, Universiti Malaysia Pahang Kuantan, 26300, Pahang, Malaysia

ARTICLE INFO

Article history:
Received 2 June 2023
Accepted 12 August 2023
Available online 16 August 2023

Keywords:
Foamed concrete
Calcium carbonate nanoparticles
Mechanical properties
Durability properties
Scanning electron microscope

ABSTRACT

Researchers have shown significant interest in the incorporation of nanoscale components into concrete, primarily driven by the unique properties exhibited by these nanoelements. A nanoparticle comprises numerous atoms arranged in a cluster ranging from 10 nm to 100 nm in size. The brittleness of foamed concrete (FC) can be effectively mitigated by incorporating nanoparticles, thereby improving its overall properties. The objective of this investigation is to analyze the effects of incorporating calcium carbonate nanoparticles (CCNPs) into FC on its mechanical and durability properties. FC had a 750 kg/m^3 density, which was achieved using a binder-filler ratio of 1:1.5 and a water-to-binder ratio of 0.45. The CCNPs material exhibited a purity level of 99.5% and possessed a fixed grain size of 40 nm. A total of seven mixes were prepared, incorporating CCNPs in FC mixes at the specific weight fractions of 0% (control), 1%, 2%, 3%, 4%, 5%, and 6%. The properties that were assessed included the slump, bulk density, flexural strength, splitting tensile strength, compressive strength, permeable porosity, water absorption, drying shrinkage, softening coefficient, and microstructural characterization. The results suggested that incorporating CCNPs into FC enhanced its mechanical and durability properties, with the most optimal improvement observed at the CCNPs addition of 4%. In comparison to the control specimen, it was witnessed that specimens containing 4% CCNPs demonstrated remarkably higher capacities in the compressive, splitting tensile, and flexural tests, with the increases of 66%, 52%, and 59%, respectively. The addition of CCNPs resulted in an improvement in the FC porosity and water absorption. However, it also led to a decrease in the workability of the mixtures. Furthermore, the study

* Corresponding author.
** Corresponding author.
*** Corresponding author.
E-mail addresses: azree@usm.my (M.A. Othuman Mydin), jaga.86@gmail.com (P. Jagadesh), alireza.bahrami@hig.se (A. Bahrami), a.f.dulaimi@uowa.edu.iq (A. Dulaimi), yozkilic@erbakan.edu.tr (Y.O. Özkılıç), mustafa_albakri@unimap.edu.my (M.M. Al Bakri Abdullah), ramadhansyah@ump.edu.my (R.P. Jaya).

https://doi.org/10.1016/j.jmrt.2023.08.106

provided the correlations between the compressive strength and splitting tensile strength, as well as the correlations between the compressive strength and flexural strength. In addition, an artificial neural network approach was employed, utilizing *k*-fold cross-validation, to predict the compressive strength. The confirmation of the property enhancement was made through the utilization of a scanning electron microscope.

1. Introduction

The expansion of concrete structures in the construction sector is an emerging trend when compared to the progress made in masonry and wood structures [1–8]. Nevertheless, due to the numerous benefits associated with concrete materials, including exceptional strength properties, good flowability, excellent fire resistance, superior thermal and insulation properties, and high impact resistance, it has gained widespread acceptance and utilization in building construction and infrastructure projects worldwide [9–13]. Concrete has been widely used thanks to its numerous advantages, resulting in a noticeable growth rate of concrete structures in comparison to other types of structures [14–18]. Additionally, frequent improvements are being conducted [19–23]. It has created considerable impacts on the expansion and improvement of human civilization during the course of human history [24–26]. Foamed concrete (FC) is widely recognized as a significant material for use in the global construction industry [27–29]. In comparison to traditional construction materials, FC has the potential to offer enhanced performance and cost-effectiveness in multiple applications [30].

FC can be characterized as a lightweight material with a porous or cellular structure, possessing the ability to flow freely. It exhibits versatility and can be effectively utilized in a diverse range of applications [31]. FC may have varying densities, typically falling within the range of 450–1950 kg/m^3. Its compressive strength ranges from 1 MPa to 20 MPa [32–35]. However, despite its growing acceptance in the construction industry, FC does have certain drawbacks. These include its high permeability, increased shrinkage, brittle nature, and a greater risk of cracking due to its permeable structure and the presence of voids. These limitations restrict its use in load-bearing applications within the building construction, as highlighted by various studies [36–38]. Numerous investigations have suggested that FC may exhibit volatility, particularly in situations where density experiences a decrease. However, even slight variations in FC density can considerably impact the durability of FC. The reduction in FC density resulted in a significant increase in the number of larger-sized voids [39]. Furthermore, it has been observed that at low densities, FC shows a high susceptibility to fracture [40]. The use of nanoparticles is not a new concept in either the realm of nature or scientific research [41]. The development of new measurement and visualization technologies has led to remarkable progress in the testing and characterization of nanoscale materials. As a result, nanotechnology has experienced a notable expansion in various industries including polymers, concretes, plastics, electronics, and medicine [42–45]. Various techniques are implemented to improve the characteristics of supplementary cementitious materials [46].

Nanomaterials represent a relatively recent advancement in the field of material science, with their conceptualization dating back to the early 1980s [47]. The term nanomaterial pertains to materials that possess a thin structure and exhibit particle sizes within the range of 1–100 nm [48]. These substances are frequently located in the transitional region between atomic masses and macroscopic bodies and encompass a diverse array of powdered materials. Nanomaterials are characterized by their small particle mass and significant specific surface area [49]. The proportion of surface atoms is 20%, which remains consistent even when the fragment size is as small as 20 nm. When compared to conventional granular materials, ultrafine powder exhibits a diverse array of exceptional characteristics [50]. Due to their remarkable efficacy, nanomaterials have emerged as a prominent area of investigation within the scientific community and are regarded as a potential catalyst for the next industrial revolution [51]. The favorable performance of ultrafine particles in concrete is largely attributed to the continuous filler of cementitious material composition [52]. Silica fume enhances the strength and durability of cement-based materials owing to its smaller granule size and higher activity level [53]. However, both the production and price of the product are relatively affordable. The field of nanotechnology has led to the development of nanomaterials as a potential substitute for silica fume, addressing the increasing demand for high-performance concrete [54]. Nanomaterials are being increasingly employed in concrete production due to their distinct nano impacts [55].

The utilization of nanoparticles has previously demonstrated a substantial improvement in durability characteristics and mechanical performance [56]. The use of appropriate nanoparticles has the potential to improve both the firmness and properties of FC simultaneously [57]. The incorporation of nanoparticles into concrete has resulted in enhancements for the material's workability, mechanical properties, durability, and microstructure, as evidenced in the available literature [58]. Various nanomaterials are commonly employed to increase the structural integrity of conventional concrete. Some notable examples include titanium oxide, carbon nanotubes, silicon dioxide, calcium carbonate, aluminium oxide, limestone, and iron oxide [59]. Due to the remarkable pozzolanic activity exhibited by calcium carbonate nano particles (CCNPs), they

have been successfully used as a substitute for traditional silica fume in various cement-based products [60]. CCNP is classified as one of several types of nanomaterials. The formation of calcium silicate hydrate (C-S-H) gel occurs through the reaction of calcium hydroxide present between the filler and binder. This process improves the strength property by leveraging the increased activity of CCNPs [61]. Recently, there has been a considerable amount of research conducted on the utilization of nano-modified concrete. Numerous studies have revealed that nanoparticles significantly contribute to the enhancement of concrete properties. They can reduce the amount of cement used to a noticeable extent and also fill the voids in the materials, thereby enabling them to have an effective influence on enhancing the performance of traditional concrete [62].

In comparison to various other nanoparticles, it has been observed that CCNPs are more cost-effective and can be obtained in significant quantities [63,64]. Prior studies have indicated that the generation of CCNPs could potentially be achieved by a plant through the utilization of waste carbon dioxide (CO_2). In their study, Batuecas et al. [65] provided a summary illustrating that the addition of 2% CCNPs results in a reduction of CO_2 emissions by approximately 69%. CO_2 emissions of the cement plant have been successfully reduced from 0.96 to 0.30 CO_2 equivalent per kilogram. Therefore, the use of CCNPs yields two substantial outcomes from both economic and environmental viewpoints. In a recent study done by Poudyal et al. [66], it was discovered that the utilization of CCNPs led to enhanced early and late-age strengths of concrete. A previous study carried out by the authors presents comprehensive testing results on cement containing different weight fractions of CCNPs [67]. It was determined that a weight fraction of 1% CCNP yielded optimal outcomes, characterized by enhanced durability and strength properties. In contemporary times, it is crucial to establish a correlation between the mechanical properties of concrete and the mix design through the employment of diverse methodologies. These relationships offer valuable insights for researchers, academics, and professionals in the industry.

1.1. *Research gap*

Research has been conducted on the utilization of CCNPs in conventional concrete, and the findings indicate that CCNPs significantly contribute to the improvement of concrete properties. The application of CCNPs in FC exhibits some limitations, thereby necessitating a comprehensive exploration of their impact on various properties. The existing literature reveals inadequate exploration of the interrelationship between the mechanical and durability properties of CCNP blended FC, hence restricting the comprehension of their interaction.

1.2. *Research objectives*

Although the effects of nanomaterials on the properties of concrete are well-understood, there has been little research on the impact of nanoparticles on the mechanical and durability properties of FC. The addition of CCNPs to concrete has been investigated, but there are still several uncertainties regarding the mechanism by which CCNPs may alter the properties of FC. This ambiguity requires clarification. Consequently, this research is an effort to address this need. The objective is to assess the effect of CCNPs addition on the mechanical and durability properties of FC. The investigation is expanded to propose a model between the mechanical and durability properties.

2. Materials and methods

Five main ingredients were required for producing the FC specimens in this study. The FC mixes contained ordinary Portland cement (OPC) as the binder, fine aggregate as the filler, clean water, a protein-based foaming agent, and CCNPs as the additive.

2.1. *Materials*

The use of CEM-1 class cement, which complies with the specifications outlined in BS-EN 197–1 [68], is suitable for a wide range of applications in the construction industry. These applications include the production of mortars for floor screeds, brickworks, and blockwork joints, as well as the preparation of interior and exterior renders. Table 1 presents the chemical compositions of cement CEM-1 employed in this study, while Table 2 provides a summary of its physical qualities.

The properties of mortar slurry are influenced by both the characteristics of sand and the composition of mixture. The gradation curve depicting fine sand utilized in this experiment is presented in Fig. 1. The determination of particle size distribution was conducted using the ASTM C33-03 standard [69]. The density of sand particles, as stated in ASTM C128-15 [70], was recorded as 2.49 g/cm^3. The sample had a fine grain composition, with 2.69% of the grains falling within the specified size range, with a maximum diameter of 5 mm. The given data had a uniformity value of 2.71 and a curvature coefficient of 1.11. Tap water was used for mixing, by the specifications provided in BS-EN 3148 [71].

To reduce the apparent friction of a solution and increase the firmness of foam, a protein foaming agent was used. The properties of the employed protein foaming agent are summarized in Table 3. As protein peptide bonds dissolve, additional hydrophobic molecules are released. When the apparent friction of the solution decreases, an interface is created for air bubbles to form, and the hydrogen bonds between chemical groups aid in the formation of stable bubbles. In comparison to air voids produced using a synthetic foaming agent, the air bubbles formed by this method

Table 1 – CEM-1 cement chemical composition.

Oxides elements	Percentage (%)
SiO_2	20.87
CaO	62.98
MgO	1.88
SO_3	3.12
Fe_2O_5	3.62
Al_2O_3	4.59
Insoluble residue	1.38
L.O.I	1.56

Table 2 – CEM-1 cement physical properties.

Properties	Values
Initial setting time	101 min
Final setting time	209 min
Consistency	25.1%
Specific gravity	3.13
Specific surface	2422 cm^2/kg

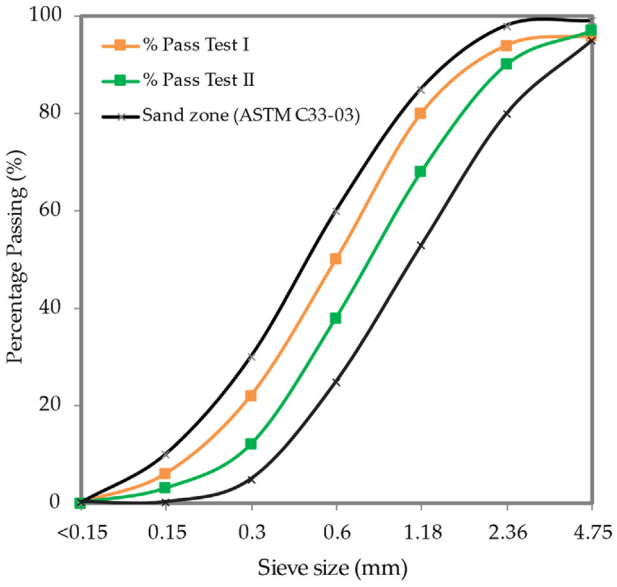

Fig. 1 – Gradation curve of fine sand.

would be more stable and smaller [72]. The protein foaming agent was applied at a 1:35 ratio with clean water. To achieve a consistent foam, a solution consisting of 1 L of protein-based foaming agent was mixed with 35 L of water. A foam generator was utilized. The foam generator had a calibrated foam nozzle with the set foam discharge rates ranging from 5 ft^3/min to 15 ft^3/min subject to the flow rate.

CCNPs utilized in this investigation were provided from a local supplier. Tables 4 and 5 present a comprehensive overview of the physical attributes and chemical compositions of CCNPs.

2.2. *Mix design*

FC density of 750 kg/m^3 was prepared for the experiments. Table 6 lists the mix proportion of FC which contain varying weight fractions of CCNPs. The binder-filler ratio was maintained at 1:1.5 and the water-binder ratio was set at 0.45. Seven FC mixes in total were produced as the control FC (no inclusion of CCNPs), and CC1, CC2, CC3, CC4, CC5, and CC6 representing varying weight fractions of 1%–6% CCNPs addition to FC, respectively.

Table 3 – Properties of foaming agent.

Properties	Descriptions/Values
Type	Protein-based
Product designation	Noraite PA-1
Color	Brown
Foam density (kg/m^3)	75 ± 5
Acidity (pH)	6.45
Specific gravity	1.12
Expansion ratio	14x
Suitable FC density (kg/m^3)	>700

Table 4 – Physical properties of CCNPs.

Properties	Values
Nanoparticles grain size (nm)	40–60
Purity (%)	99
Density (g/cm^3)	2.89
Color	White
Molar mass (g/mol)	100.09

2.3. *Production of FC*

The process of producing FC on a small scale is relatively straightforward, requiring neither costly nor complicated machinery. In fact, in many instances, existing equipment used for conventional concrete production can be used. In this study, a low-density FC was produced with a constant dry density of 750 kg/m^3 by controlling the foam content added to cement slurry. There were variations in CCNPs addition specifically 0% (control), 1%, 2%, 3%, 4%, 5%, and 6%. A maximum of 6% weight fraction of CCNPs was selected to avoid FC with reduced density. Firstly, a dry mixture of cement, sand, and CCNPs was mixed for 3 min in a 0.2 m^3 capacity tilting concrete mixer. Then, the dry mix was blended with water for an additional 3 min. The production of FC necessitates the presence of an aqueous stable foam, which is considered a crucial component. The foaming generator serves as a medium through which the liquid chemical transforms into a state of stable foam. Therefore, a Portafoam TM-2 machine connected to a premix solution tank (Fig. 2) was used to generate the foam, as illustrated in Fig. 1. A premix solution tank-producing system is ideal for use in conjunction with batching equipment. Since just a small amount of foam was needed, it was incredibly cost-effective. Foam liquid concentrates and water were premixed in the tank using pressure tank-producing equipment. The solution was then expelled from the pressure tank through the foam-producing nozzle. The procedure was done only by air pressure. The pressure tank had a capacity of 40 L while calibrated foam nozzles for the pressure tank system were available. This

Table 5 – Chemical compositions of CCNPs.

Oxides elements	Percentage (%)
CaO	77.29
Fe_2O_3	0.05
SiO_2	0.59
P_2O_5	0.01
Al_2O_3	0.08
SO_3	0.01
K_2O	0.01
MgO	0.14
TiO_2	0.01
Na_2O	0.01
L.O.I	21.8

Table 6 – Mix proportions of FC-CCNP composites.

FC coding	CCNP (%)	CCNP (kg/m^3)	Binder (kg/m^3)	Filler (kg/m^3)	Water (kg/m^3)	Foam (kg/m^3)
Control	0	0.0	284.4	426.6	128.0	38.5
CC1	1	8.8	284.4	426.6	128.0	38.5
CC2	2	17.5	284.4	426.6	128.0	38.5
CC3	3	26.3	284.4	426.6	128.0	38.5
CC4	4	35.1	284.4	426.6	128.0	38.5
CC5	5	43.9	284.4	426.6	128.0	38.5
CC6	6	52.7	284.4	426.6	128.0	38.5

foam generator would also automatically combine liquid foam concentrate with water and compressed air in predetermined quantities. It would suction liquid foam concentrate constantly from the concentrate's container. The liquid foam concentrate was metered and blended with water to make a premixed solution with the appropriate concentration ratio to achieve the required FC density. An air compressor was then utilized to pressurize and balance the solution. This compressor's air and the premixed solution were then metered via a nozzle, the output of which was controlled by the foam generator. The nozzle was intended to produce a fine micro-bubbled foam of a certain density and quantity. To measure its density, a 5-L container was used and the density of the foam should be between 70 kg/m^3 and 80 kg/m^3. Once the density was confirmed to be within the acceptable range, it was inserted into the mortar slurry mix and the mixer was run for a few more minutes until there was no noticeable foam left in the drum. According to ASTM C 1437 [73], a flow table test was conducted to determine the consistency of newly mixed FC. Then, the homogenous FC mix was placed in steel molds. A plastic sheet was placed over the molds for 24 h to protect them from moisture. The samples were cured by moisture curing as soon as they were demolded until they were ready for testing.

2.4. *Experimental procedure*

Various tests were done to evaluate the mechanical and physical properties of FC, including the flexural strength, compressive strength, splitting tensile strength, porosity, slump flow rate, and water absorption. A prism with the dimensions of 100 mm × 100 mm × 500 mm was utilized to perform the flexural tests, following the guidelines outlined in the BS-EN 12390-5 standard [74]. The compression tests were conducted using FC cubes measuring 100 mm × 100 mm × 100 mm, by the specifications mentioned in the BS-EN 12390–3 standard [75]. Subsequently, a cylindrical specimen with a diameter of 100 mm and a height of 200 mm was employed to determine the splitting tensile strength. The splitting tensile tests adhere to the guidelines specified in the BS-EN 12390–6 standard [76].

The investigation also included an assessment of the water absorption and porosity properties of FC. The softening coefficient is a significant indicator used to characterize FC. The softening coefficient pertains to the capacity of a specific FC mixture to withstand the water damage, and it exerts a notable impact on materials characterized by elevated levels of the water absorption and porosity. The softening coefficient was determined based on the high water absorption and porosity of FC. It was calculated as the ratio of the compressive strength of FC when saturated with water to its compressive strength in a dry condition.

Furthermore, the porosity of FC was evaluated using a vacuum saturation technique [77], and a water absorption test was accomplished by the BS-EN 1881-122 standard [78]. In accordance with the ASTM C878/C878M–22 standard [79], a drying shrinkage test was conducted to determine the volumetric contraction of FC due to the moisture loss. This test involved the use of a prism measuring 75 mm × 75 mm × 290 mm. Besides, the workability test was also carried out in agreement with ASTM C 230–97 [80].

3. Results and discussion

3.1. *Slump*

The slump flow must be taken into account when evaluating the FC performance. The workability of FC-CCNP composites in relation to the slump value is depicted in Fig. 3. As seen in Fig. 3, the slump flow of the FC blends decreased as the CCNP content

Fig. 2 – A Portafoam TM-2 machine was utilized to produce stable foam.

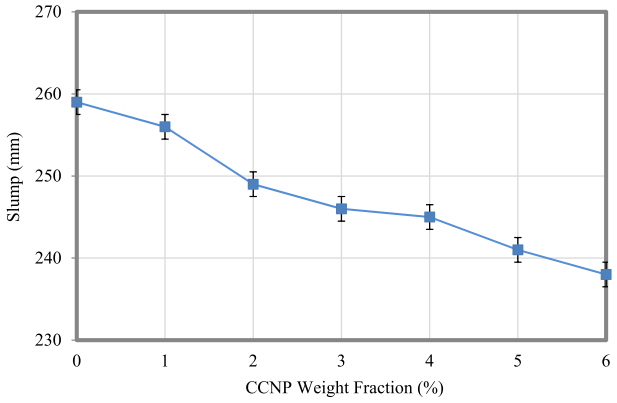

Fig. 3 – Slump of FC-CCNP composites.

increased. The control FC achieved the greatest slump flow diameter of 259 mm, while FC with 6% CCNPs recorded the smallest slump flow diameter of 238 mm. The results were consistent with those of Supit and Shaikh [81]. Compared to the control FC, the slump flow of FC containing CCNPs reduced. As the weight fraction of CCNPs in the mixture increased, the fluidity decreased. The workability of FC containing 1% CCNP was lower than that of the control FC. The decrease in the workability of FC was due to the CCNPs' higher specific surface area. Meng et al. [82] found that the water usage increased along with the CCNPs' weight fraction. The water demand experienced the modest rises of 0.4%, 1.8%, and 3.2% depending on the CCNPs' weight fractions as 1%, 3%, and 5%, respectively. However, this influence was lessened when a CCNP intermediate slurry was employed. With the addition of CCNPs from 1% to 6%, the slump flow fell by 1.2%, 3.9%, 5.0%, 5.4%, 6.9%, and 8.1%, respectively, in comparison to the control FC. The CCNP medium slurry was faster to dissipate uniformly and might greatly improve the particle size dispersion, which was the main justification for this modification. The presence of CCNPs could accelerate setting time in addition to enhancing the cement hydration.

3.2. *Density*

The material's varying densities are influenced by a combination of several factors, including the inclusion of different types of cement, sand, foaming agent, and the incorporation

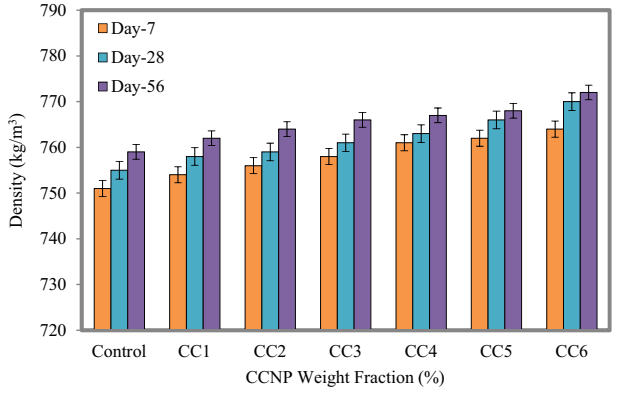

Fig. 4 – Density of FC-CCNP composites.

of an additive in the FC base mix. However, maintaining FC densities within a range of roughly ±60 kg/m^3 of their targeted final density is of utmost significance. Fig. 4 displays the relationship between the influence of varying weight fractions of CCNPs on the FC densities. The observed trend in Fig. 4 indicates that there was a slight increase in the FC density as the weight fraction of CCNP increased (from 1% to 6%) and as the curing age progressed from day 7 to day 56. On the 28th day, the FC mixture, which consisted of 6% weight percentage of CCNPs, exhibited a density of 770 kg/m^3. In contrast, the control FC gave a density of 755 kg/m^3. The FC specimen, containing 2% CCNPs, had a density of 756 kg/m^3 after 7 days of curing. Subsequently, the density increased to 759 kg/m^3 on day 28 and further rose to 764 kg/m^3 on day 28 of the curing process. On the 56th day, however, the density remained satisfactory. On day 28, the control, CC1, CC2, CC3, CC4, CC5, and CC6 specimens exhibited variations in density compared to the target values of 9, 12, 14, 16, 17, 18, and 22 kg/m^3. The density increase was attributed to the higher specific gravity of CCNPs within the FC cementitious matrix [83]. Moreover, the incorporation of CCNPs into FC has the potential to improve the density of grain filling, reduce the fraction of voids in solid fragments, and enhance the availability of free water for lubricating [84]. The plastic viscosity may increase as a consequence of these opposing mechanisms. In addition, adding CCNPs to FC has been observed to result in a rise in the water consumption, as well as higher yield stress and viscosity [85]. CCNP is used as a filler material in the FC matrix, leading to a decrease in the porosity and voids, hence enhancing the density of FC [86].

3.3. *Flexural strength*

Fig. 5 demonstrates the influence of the incorporation of different weight fractions of CCNPs on the flexural strength of FC. The results indicate an initial rise of up to 4% in the flexural strength with the addition of CCNPs. However, as the CCNPs content further increased, the flexural strength gradually declined. At the age of 28 days, the addition of CCNPs at weight the fractions of 1%, 2%, 3%, 4%, 5%, and 6% resulted in increases in the flexural strengths as 7.46%, 22.39%, 30.26%, 58.75%, 23.57%, and 2.31%, respectively. The CC4 blend exhibited a substantially greater increase in the flexural strength compared to the other mixes. An observed increase in the flexural strength was recorded for the CC4 mix, with a rate of 18.75% at 28 days and 34.38% at 56 days compared to the 7th day. This increase in the flexural strength can be attributed to the ability of the matrix material to transmit loads to CCNPs. CCNPs provide a strong bonding with the cement matrix because of their superlattice nature, characterized by enhanced van der Waals forces at the contact. Moreover, CCNP induces the formation of a compact arrangement of hydration products, resulting in a wider range of particle sizes and a decrease in the dimensions and connectivity of pores, hence improving the flexural strength. The packing density of a matrix is increased when CCNPs are incorporated into an FC cementitious matrix, leading to strengthened bonding between the filler and binder at the interfacial transition area. Moreover, the presence of non-uniformly distributed particles, caused by a critical concentration of more than 5% CCNPs in FC, may have contributed to the decline in the flexural

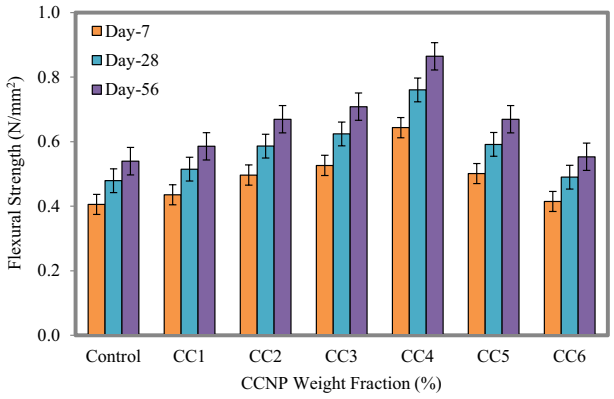

Fig. 5 – Flexural strength of FC-CCNP composites.

strength [87]. The literature suggests two possibilities for the observed rise in the flexural strength. Firstly, it implies that the presence of CCNPs fills the micropores within the cementitious matrix, resulting in an increase in the density. Secondly, the production of new hydrated components is proposed as an additional factor contributing to the enhanced flexural strength [88]. The incorporation of CCNPs at their minimum concentration leads to a notable improvement in the flexural strength. Liu et al. [89] specifically documented that the inclusion of 1% CCNP resulted in a noticeable enhancement in the flexural strength compared to the control specimen. A decrease in the flexural strength was seen at greater replacement levels, which can be attributed to the inadequate dispersion and agglomeration of nanoparticles within the cementitious composites [90].

3.4. *Splitting tensile strength*

In line with the findings on the flexural strength, it was seen that an increase in the weight fraction of CCNPs resulted in an enhancement of the splitting tensile strength of FC at 7, 28, and 56 days, as illustrated in Fig. 6. The splitting tensile strength of the specimens increased by 7%, 21%, 24%, and 52% at 28 days, and by 8%, 24%, 32%, and 52% at 7 days, when the weight fractions of 1%, 2%, 3%, and 4% CCNPs were respectively added to the specimens, as compared to the control specimen. However, following the incorporation of 4% CCNPs, there was a gradual decrease in the splitting tensile strength. The CCNP is known for its intricate nature, characterized by its nanoscopic scale, significant interfacial area, and precise atom arrangement. When exposed to external stress, the atoms exhibit rapid migration, absorb energy during this process, and demonstrate resistance to deformation. When force is exerted on FC, it results in the formation of an internal network of microcracks, ultimately leading to the fracture of FC. This fracture is portrayed by the presence of numerous small and major cracks. The emergence, growth, and coalescence of internal fractures have a detrimental effect on the load-bearing surface of the FC matrix. The reduction in the effective load-bearing area also leads to an increase in the stresses at major fracture points. The presence of CCNPs enhances the fracture resistance and mitigates the crack propagation. CCNPs possess a considerable aspect ratio and shape that enable them to effectively obstruct and redirect microcracks, thereby exhibiting robust properties for inhibiting the crack advancement [91]. Additionally, the bridging function of CCNP particles can effectively prevent and mitigate the propagation of fractures. Certain fractures tend to naturally close when subjected to the compressive pressure, however, the occurrence of crack merging becomes more prominent when exposed to the tensile strain [92]. Although the addition of CCNPs to FC beyond 4% showed a decreasing trend, it is noteworthy that the splitting tensile strength at the weight fractions of 5% and 6% CCNPs was still 17% and 7% higher, respectively, compared to the control FC on day 28.

3.5. *Compressive strength*

In accordance with Fig. 7, there is a positive correlation between the weight percentage of CCNPs and the compressive strength of FC. The compressive strength of FC was improved as the weight fraction of CCNPs increased, with the highest value observed at an optimal weight fraction of 4%. The addition of 6% CCNPs experienced an increase of 14.3% in the compressive strength. The inclusion of 4% weight fraction of CCNPs resulted in a notable enhancement of the compressive strength as 3.36 MPa. This improvement represents remarkable 66% increase compared to the control FC. Within the FC cementitious matrix, these elements collaborate synergistically to enhance the compressive strength. The inclusion of

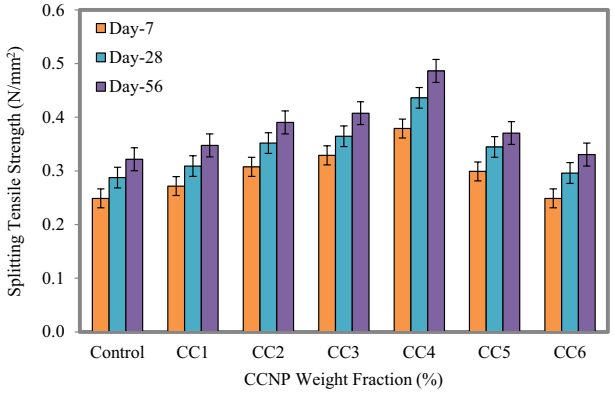

Fig. 6 – Splitting tensile strength of FC-CCNP composites.

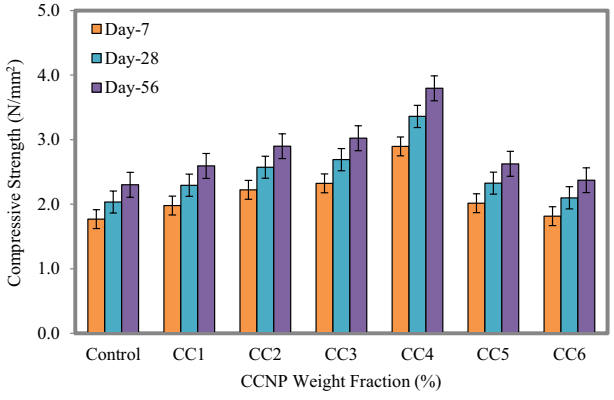

Fig. 7 – Compressive strength of FC-CCNP composites.

5% concentration of CCNPs resulted in 15% increase in the compressive strength compared to the control sample. This enhancement is lower than that observed with the addition of 3% CCNPs. Nanoparticles with high specific areas are vulnerable to clustering due to secondary interactions [93]. There was an increase in the compressive strength of the specimens when CCNPs were added at different weight fractions. Specifically, there were increases of approximately 12.78%, 26.52%, 32.27%, 65.18%, 14.38%, and 3.19% when CCNPs were added at 1%, 2%, 3%, 4%, 5%, and 6%, respectively, compared to the control specimen FC. These results were obtained after conducting a 28-day testing of the FC specimens. Additionally, it was seen that the compressive strength rate increased for a duration of 28 days when compared to a duration of 7 days. The inclusion of CCNPs in FC leads to the production of minerals such as calcium silicate hydrate (C–S–H) and calcium aluminate silicate hydrate (C-A-S-H), which play a significant role in enhancing the mechanical properties. In addition, CCNPs are utilized as filler material to enhance the density and subsequently improve the strength properties. The increase in the compressive strength can be attributed to the accelerated reaction rate of tricalcium aluminate, resulting in the production of a greater amount of carbon aluminate complex. Consequently, this leads to an increase in the hydration compounds [94]. Furthermore, the nanoparticles of CCNPs exhibit a reactive behavior when interacting with tricalcium silicate, resulting in an enhanced rate of hardening and development of FC. This effect is particularly noticeable when the replacement level is lower and during the early stages of the FC strength. The reaction of tricalcium aluminate and tricalcium silicate with CCNPs leads to the formation of a considerable quantity of hydration products. These products consume the available water, effectively counteracting the dilution effect of the bonded materials. Consequently, this process contributes to an increase in the strength. The inadequate dispersion of CCNP particles and the presence of van der Waals forces in the binder can be identified as factors contributing to the achievement of an optimized level of CCNPs.

3.6. *Porosity*

The results of the permeable porosity of FC-CCNP composites are depicted in Fig. 8. The increase in the weight percentage of CCNPs in the FC mixes resulted in a decrease in the permeable porosity. The inclusion of 3% and 4% CCNPs in the control FC resulted in an enhancement of the permeability porosity by 6% and 9%, respectively, when compared to the control FC. The introduction of CCNPs into the pores at the interface between the binder paste and the filler caused a decrease in the activity of the capillary pores. It is important to note that the pores were filled with CCNPs. The observed trend in the permeability porosity values can be attributed to the alteration of the microstructure in the presence of CCNPs. These CCNPs hold together to form a gel chain by acting as kernels, and this is one of the reasons why such a trend can be seen in the permeable porosity values [95]. CCNPs are employed to address the discrete and continuous gaps observed in the specimens, resulting in a reduction of the capillary suction that facilitates the water absorption into the FC specimens.

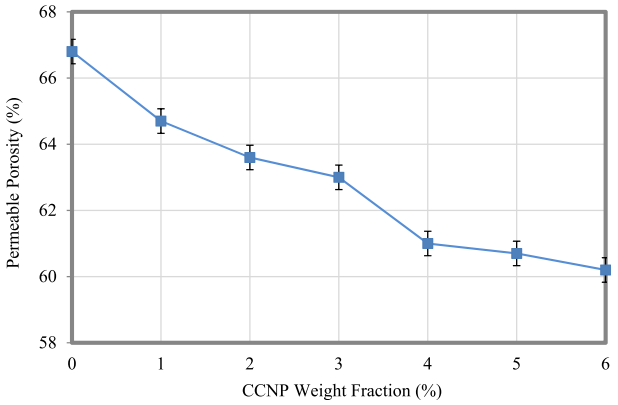

Fig. 8 – Permeable porosity of FC-CCNP composites.

This effect involves a reduction in the size of the biggest pores on the outer surface as a result of the production of newly hydrated compounds, which is attributed to the increase in the content of CCNPs. As previously mentioned, it has been indicated that CCNPs exhibit involvement in the hydration reaction, hence facilitating the hydration process of various cementitious materials. Additionally, CCNPs effectively occupy voids within the cement matrix, reducing the pore volume [96].

3.7. *Water absorption*

Fig. 9 displays the outcomes of the water absorption of FC-CCNP composites. The water absorption gradually decreased as the CCNP content increased. The water absorption value of the control FC was 25.8%. 6% weight fraction of CCNPs in FC demonstrated a significant decrease in the water penetration when compared to all other weight fractions of CCNPs. This is so that the FC mixture's gel pores can be sealed off owing to the lower particle size. With the addition of 6% CCNPs, the water absorption capacity was determined to be 22.9%, which is a decrease of nearly 11% from the control specimen. The reason is due to the densified microstructure and refined pores. With 4% addition of CCNPs, a considerable decrease in the water absorption from the control specimen to FC-CCNP composites was apparent. This effect also occurs with greater weight fractions of CCNPs in FC. Above the 4% weight

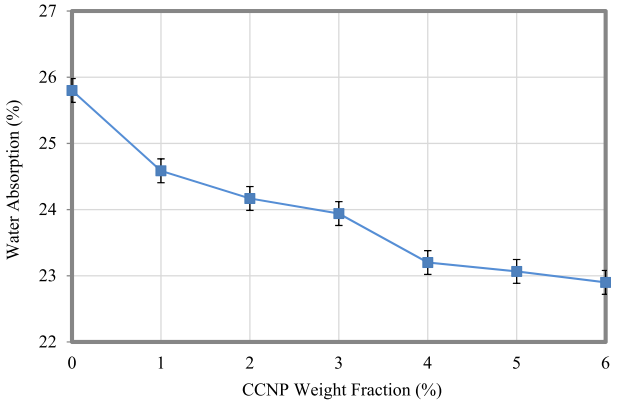

Fig. 9 – Water absorption of FC-CCNP composites.

fraction of CCNPs in FC, the decrease in the water absorption capacity was minimal. An increase in CCNPs decreaseed the water absorption because it increased the hydration products, absorbed more calcium hydroxide, and caused the formation of new gels to fill the matrix's gaps, decreasing the porosity of FC [97].

3.8. Drying shrinkage

The drying shrinkage of FC is a phenomenon characterized by a decrease in volume primarily owing to the evaporation of water from FC in conditions of the low ambient humidity. This particular type of shrinkage is widely recognized as a leading cause of concrete cracking. The cement paste used in FC is considered to exhibit viscoelastic behavior, meaning that its volume change is influenced by both elastic and viscous mechanisms. The results of the drying shrinkage of FC-CCNP composites are presented in Fig. 10. As shown in Fig. 10, the drying shrinkage exhibited an increase over time for all the mixtures. Overall, the control mix gave the greatest degree of the drying shrinkage. The incorporation of CCNPs in FC resulted in a substantial reduction in the drying shrinkage. The presence of 4% CCNPs in the FC mix (mix CC4) led to the attainment of the optimal outcome. CCNPs exhibit the ability to absorb the tensile energy while the FC material undergoes the shrinkage. This energy transfer occurs at the interface between CCNPs and the FC matrices, resulting in the dispersion of energy to the adjacent matrix. Consequently, the concentration of the tensile stress within the FC matrix decreases, thereby enhancing its resistance to the crack propagation. According to Abellan-Garcia et al. [98], when the weight fraction of CCNPs in the FC matrix exceeds 4%, inadequate dispersion of CCNPs within the FC matrix results in the agglomeration of nanoparticles. Consequently, this phenomenon impedes the ability of CCNPs to effectively disperse the tensile stress from the FC region to other areas via its surface. This explanation provides support for the assertion that there is no substantial enhancement in the resistance to the drying shrinkage cracking beyond a weight fraction of 4%. When a suitable weight proportion of CCNPs is uniformly distributed within the cement paste composed of FC, the resulting hydrated cement products tend to accumulate around CCNPs. This phenomenon can be attributed to the higher surface energy of CCNPs, which serves as a favorable site for nucleation.

3.9. Softening coefficient

If FC-CCNP composites undergo the water absorption and possess inadequate water resistance, it will significantly hinder the expected lifespan of FC as an insulation material. The softening coefficient is a substantial consideration that distinguishes the water resistance properties of cement-based materials. It is expressed as the proportion of the compressive strength of FC when saturated with water to the compressive strength of FC when it is in a dry state. Fig. 11 shows the softening coefficient of FC-CCNP composites. The data presented in Fig. 11 illustrate that the softening coefficient is consistently below 1.00 across all FC-CCNP mixtures. This indicates that the presence of water saturation had a detrimental impact on the compressive strength of FC-CCNP composites. The experimental results demonstrated an upward trend between the weight fraction of CCNPs and the softening coefficient of FC-CCNP composites, up to a weight fraction of 4% (referred to as mix CC4). The mix CC4 displayed the highest softening coefficient of 0.94, in contrast to the control mix which had the lowest softening coefficient of 0.85. For CC5 and CC6 mixes, the softening coefficient decreased slightly to 0.91 and 0.90, respectively, when exceeding 4%. In general, it is recommended that the softening coefficient of water-resistant materials, such as FC, should be more than 0.85 [99]. Hence, based on the softening coefficient obtained in this research, it is justifiable to assert that all FC-CCNP composites examined in this investigation exhibited a good level of the water resistance capability. The relationship between the water resistance of a material and its pore structure and particle adhesion method is widely acknowledged in the literature [100]. Accordingly, the reduction of the porosity in FC is a crucial method for enhancing its mechanical properties.

3.10. Microstructural study

Fig. 12 displays the scanning electron microscope (SEM) images of the control FC in comparison to the FC containing

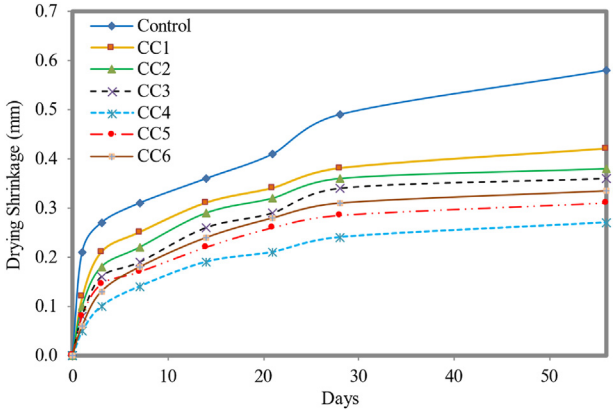

Fig. 10 – Drying shrinkage of FC-CCNP composites.

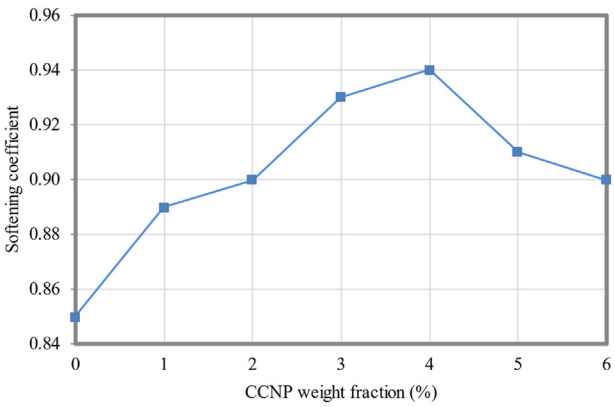

Fig. 11 – Softening coefficient of FC-CCNP composites.

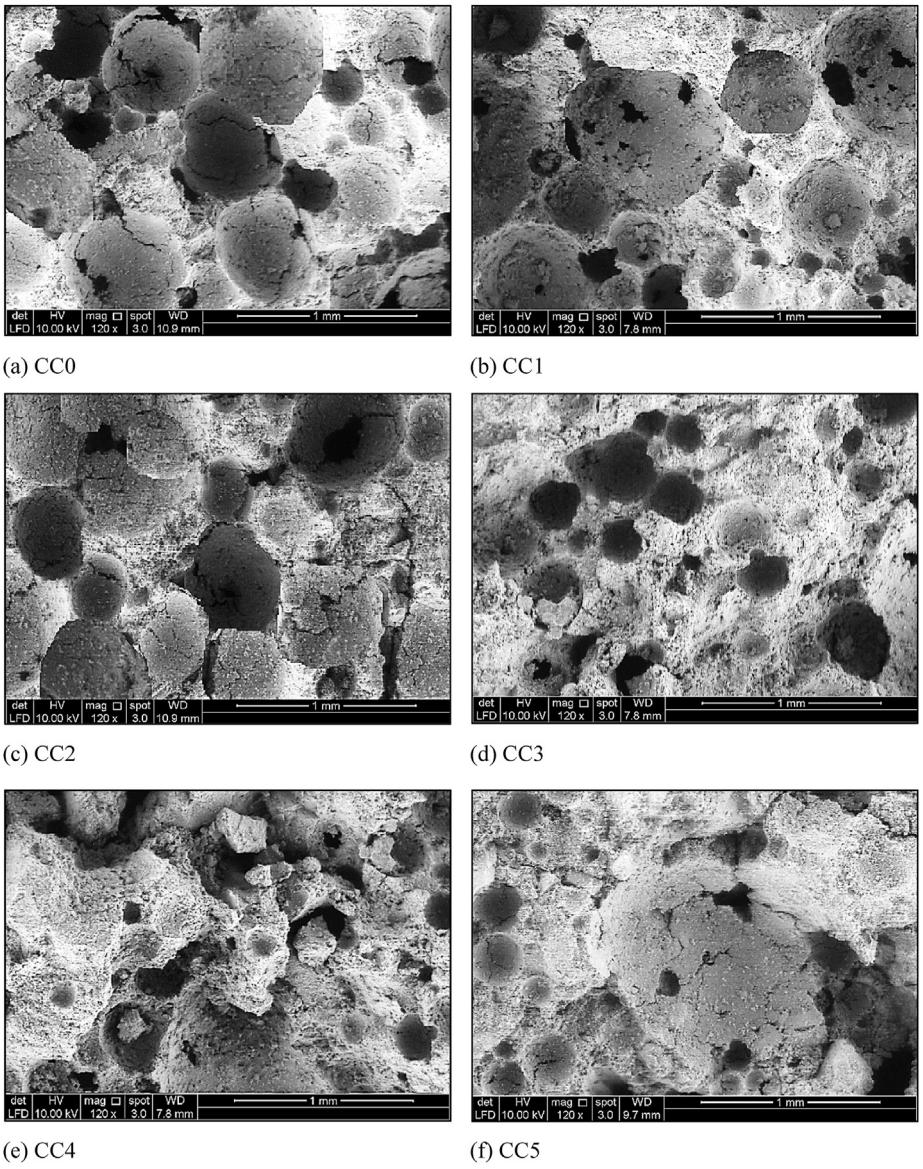

Fig. 12 – SEM micrographs.

various weight fractions of CCNPs. The control FC (as shown in Fig. 12a) exhibits greater void sizes and connected pores. The inclusion of CCNPs in the composition of the base mixture resulted in a considerable reduction in void sizes, as depicted in Fig. 12b–f. In addition to the aforementioned point, the presence of CCNPs led to an increase in the density of the matrix as a result of the enhanced development of C–S–H. This occurrence is confirmed by the observed enhancements in both density and strength properties. The strength of FC was augmented by the widespread dispersion of C–S–H gel within the cementitious matrix that had been hydrated with FC. The presence of $Ca(OH)_2$ and $CaCO_3$ was found on the external surface of the hydrated FC cement paste. The strength of the mixture was notably increased as a result of the expansion and dispersion of mineral elements. The control FC exhibited a pore diameter of 0.69 mm. However, upon the introduction of 1% CCNP, the pore size decreased to 0.66 mm, suggesting the presence of newly formed hydration compounds. Furthermore, with the inclusion of CCNPs, the void size was decreased to 0.53 mm for the CC3 mixture. Moreover, for the 3% concentration of CCNPs, the void size was further reduced to 0.39 mm. This suggests that an increase in the incorporation of CCNPs leads to a greater generation of hydration products. Additionally, the inclusion of CCNPs resulted in filling of the pores, thereby raising the density of the mixture. The CC4 mix had an optimal mix proportion, characterized by a void size of 0.26 mm, which suggests a higher concentration of hydration products and pore filling. This led to an increase in the density. In a study conducted by Martinez-Garcia et al. [101], it was demonstrated that the production of hydrated products gave a reduction in the void size, which was consistent with previous findings. The introduction of new products also contributed to this effect. In addition to 4% increase in the content of CCNPs, a layer

composed of hydrated cementitious materials, specifically portlandite and calcite, was placed on top of the compacted cement matrix. The lack of calcium in the combination may have hindered the breakdown of C–S–H. The decreased strength of the CC5 mix can be ascribed to the insufficient mineral element development inside the composite. The decreased indication and dispersion of C–S–H can be attributed to the presence of unreacted particles in the supplementary substance. The C–S–H gel experienced a significant breakdown, leading to the formation of calcite crystals. The diminished strength of CC5 was noted as a result of the existing microstructural circumstances. In addition, it was observed that the composite had inadequate mechanical properties, and the chemical interaction between the portlandite and silica content ceased after a period of 28 days.

According to the observations made in Fig. 12, it can be noticed that the equidimensional spherical nanoparticles were accompanied by rhombohedral crystals at the nanoscale. The production of calcite was reported by Jagadesh et al. [102]. The reaction between tri-calcium aluminate and gypsum results in calcium sulfoaluminates or ettringite and thereby the reduction of gypsum. The conversion of calcium sulfoaluminates to monosulfoaluminates was necessitated by the unavailability of gypsum. The transformation of monosulfoaluminates is modified with the incorporation of CCNPs. The carbonates present in the CCNP cement experience a chemical reaction with tri-calcium aluminate in FC, resulting in the formation of calcium carbon-aluminates. The inclusion of CCNPs results in the substitution of sulphate ions in calcium sulfoaluminates and monosulfoaluminates with carbonate ions, hence enhancing the stability of calcium sulfoaluminates [103]. Based on Fig. 12(e), it can be inferred that a condensed arrangement characterized by a reduced presence of hydration products within the C–S–H gel, along with a lower occurrence of sulfoaluminates, leads to the development of a more tightly packed structure. Consequently, this denser matrix exhibits an enhancement in its mechanical capabilities. In accordance with the microscopic observations, it can be inferred that the formation of a denser matrix can be attributed to the existence of small C–S–H gel products and filling of the spaces by nanoparticles, thereby leading to an increase in the density.

4. Correlation analysis between properties of FC-CCNP specimens

To accurately determine the properties of FC, it is necessary to obtain information regarding its other properties or the constituents materials used in the mixture. These correlations are necessary for cost savings, environmental resource conservation, manpower efficiency, time efficiency, and other benefits for researchers, academics, and professionals in the industry. Martinez-Garcia et al. [104] reported the influence of various factors on the strength properties of concrete. Therefore, it is imperative to quantify one of the mechanical properties of FC-CCNP by estimating it from other mechanical properties. Correlation expressions have been developed to establish the relationship between the properties of FC-CCNP. The fundamental linear correlation method was employed to investigate the relationship between the physical properties and strength properties. Fig. 13 illustrates the correlation analysis conducted on the compressive and flexural strengths of FC-CCNP composites. The power relations among all the FC-CCNP specimens exhibited a strong correlation. The compressive and splitting tensile strengths exhibited a strong positive linear relationship, as evidenced by a coefficient of determination (R^2) of 0.998. In the majority of the literature pertaining to the relationship between the compressive strength and flexural strength, it is observed that a power relationship exists between these two strengths.

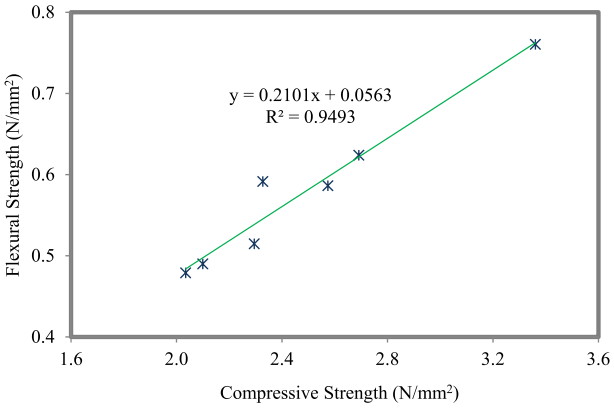

Fig. 13 – Compressive-flexural strengths correlation analysis of FC-CCNP composites.

The relationship between the compressive and splitting tensile strengths of FC-CCNP composites is presented in Fig. 14. The data distribution in Fig. 14, with an R^2 value of 0.995, provides evidence supporting the assertion of a significant relationship between the compressive and splitting tensile strength of FC reinforced by CCNPs. By the literature, there exists a correlation between the compressive strength and splitting tensile strength, which can be described as a power relationship. Fig. 15 demonstrates evidence supporting the correlation between the flexural and splitting tensile strengths of FC. Based on an R^2 value of 0.997, it is evident that a strong linear correlation exists between the two strength parameters.

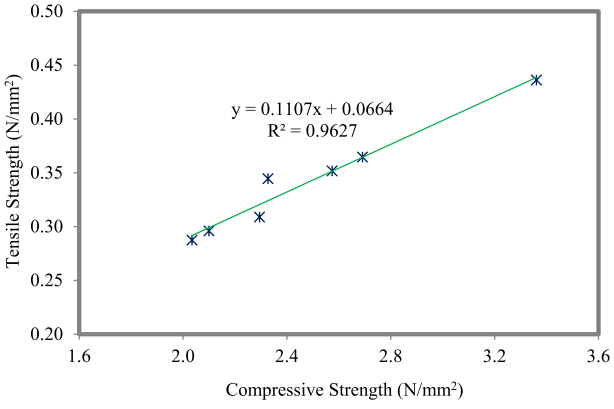

Fig. 14 – Compressive-splitting tensile strengths correlation analysis of FC-CCNP composites.

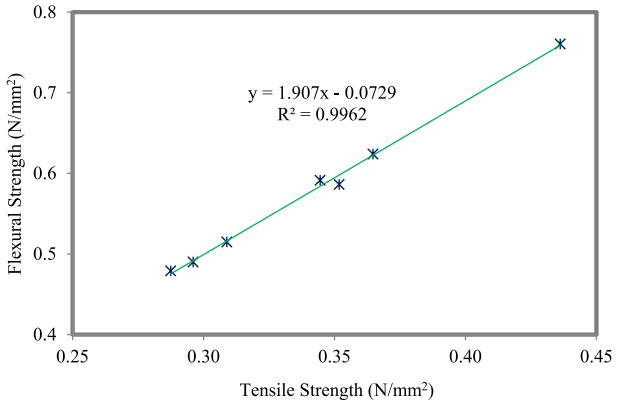

Fig. 15 – Flexural–splitting tensile strengths correlation analysis of FC-CCNP composites.

Additionally, Fig. 16 displays the correlation between the permeable porosity and water absorption of FC-CCNP composites. An R^2 value of 0.9881 was achieved. The correlation indicates that there is a positive relationship between the porosity and water absorption value, whereby an increase in the porosity led to an increase in the water absorption. The correlation expressions presented show a significant relationship between changes in the variables and corresponding changes in the response variable. Furthermore, the prediction models developed imply a substantial level of explanatory power, accounting for a noticeable proportion of the observed variability. It is important to note that the correlation expressions suggested in this study can be utilized in the design of nanoparticle-modified FC.

5. Compressive strength estimation using artificial neural network

Artificial neural network (ANN) is a machine learning model that exhibits similarities to the neural networks present in the human brain. ANN has been extensively used in various engineering applications due to their capability to effectively model intricate nonlinear systems [105]. One application chosen for the analysis in this study involves the estimation of the compressive strength of FC. To achieve an optimal blend and attain the desired level of the strength, substantial financial, temporal, and human resources are required, along with the consumption of natural resources. The ANN technique is utilized, employing the feedforward propagation method, to estimate the compressive strength of FC during a specified testing period. The compressive strength can be determined by employing a neural network architecture with the number of hidden layers set equal to the number of input variables. Fig. 17 depicts the number of layers employed for the modeling process using ANN.

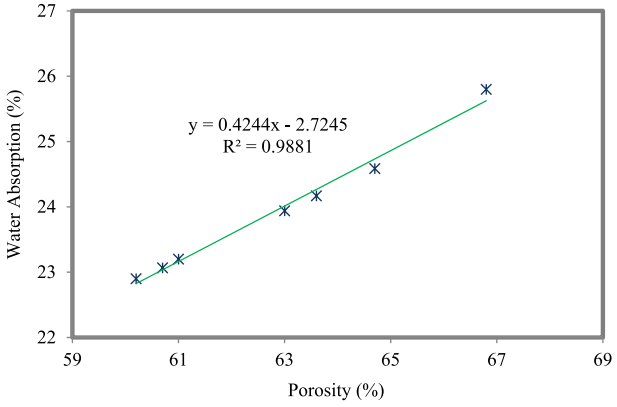

Fig. 16 – Porosity-water absorption correlation analysis of FC-CCNP composites.

A total of 182 data points were collected to develop a model for predicting the compressive strength of FC. The input variables for this study included the binder content, natural fine aggregate, water, foaming agent, and age of testing of the specimens (Table 7). The output variable being measured was the compressive strength [106].

Prior to making predictions, the data underwent preprocessing utilizing normalization techniques. This was done to ensure that the data were evenly distributed within the range of −1 to +1. It is essential to incorporate normalization methods in the pre-processing of data for machine learning. These techniques are employed to transform data into a format that can be easily processed by machine learning algorithms. Normalization can enhance the performance of machine learning models by mitigating the impact of outliers, expediting convergence, and reducing overfitting. The normalization technique utilized in this modeling is expressed in Eq. (1), specifically employing a scaling technique.

$$X_N = \left\{ \left[\frac{2(X - X_{min})}{(X_{Max} - X_{Min})} \right] - 1 \right\} \quad (1)$$

whereas X_N is the normalized data value, X_{min} is the minimum value of the observed data, and X_{max} is the maximum value of observed data from the literature. The Levenberg-Marquardt (LM) algorithm with the transform function as Tansingh was used to predict the compressive strength. A popular optimization method for training ANN is the LM algorithm. It is frequently applied to the resolution of nonlinear regression issues, including predicting the concrete's compressive strength. By minimizing the difference between the predicted output and actual output for each input-output combination in the training data, the LM algorithm was employed to optimize the weights and biases of ANN. The weights and biases in the network are modified iteratively, guided by the error between the expected output and actual output. Feedforward propagation method with the performance error as mean square error was used in this study. A hyperparameter called "epochs" determines how many times the learning algorithm

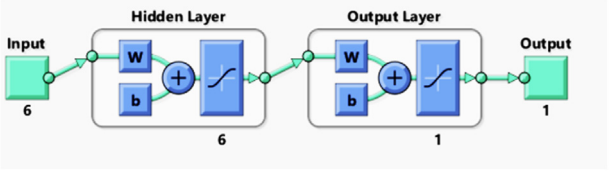

Fig. 17 – Number of layers used for modeling.

Table 7 – Variables used for ANN analysis to determine compressive strength of FC.

	Binder content (kg/m^3)	Natural fine aggregate (kg/m^3)	Water (kg/m^3)	Foaming agent (kg/m^3)	Age of testing (Days)	Compressive strength (MPa)
Maximum	600.00	1355.00	484.00	0.17	3.00	0.10
Minimum	107.20	0.00	68.90	60.00	180.00	18.50

will go through the complete training dataset. Every sample in the training dataset had a chance to change the internal model parameters once during an epoch. Epoch for the present study is illustrated in Fig. 18.

The literature data utilized the k-fold cross-validation, where the data were divided into ten subsets with approximately equal size. The neural network was trained using a total of seven sets, which accounted for 70% of the observations. The remaining three sets, comprising 30% of the observations, were set aside for evaluating the effectiveness of the model. The procedure was repeated ten times to accommodate the ten sets of the data. Seven sets were employed for the model development, while the remaining three sets were used for testing purposes. This was done using four distinct combinations. The utilization of this method offers the advantage of enabling the anticipation of the overall predictive capability of ANN. The k-fold cross-validation method, specifically using $k = 10$ folds, is a widely employed technique for obtaining accurate data models. R^2 was used to assess the performance of the model displayed in Fig. 19 for $k = 1$. The number of neurons was set to 7, which corresponds to the number of the input variables. Additionally, two hidden layers were utilized, with one serving as the input layer and the other as the output layer. Based on the findings indicated in Fig. 20, it can be concluded that the optimal value for the k -fold cross-validation was determined to be $k = 1$. This particular value exhibits the highest average R^2 value of 0.921 for both training and testing.

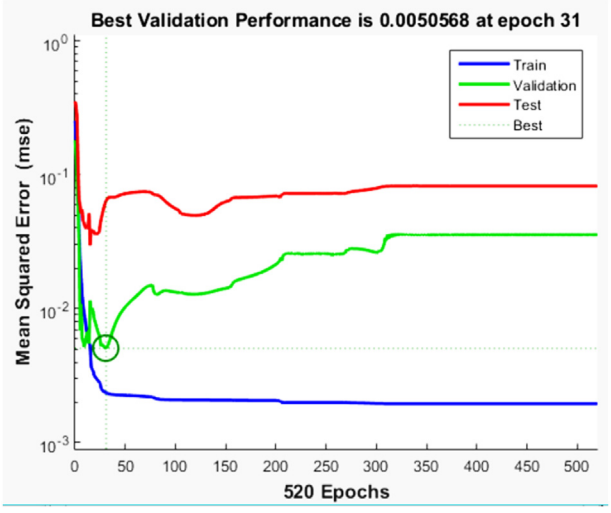

Fig. 18 – Epochs for ANN model to predict compressive strength.

Fig. 20 depicts the predicted compressive strength of FC-CCNP composites. It has been determined that the input parameters exhibit a significant relationship. The predicted compressive strength was determined by utilizing the weights and biases obtained through the implementation of the ANN technique. Eq. (9) is utilized for the estimation of the normalized compressive strength, while the denormalized value is obtained. Eq. (2) to Eq. (8) are used for the estimation of the constant value ranging from E1 to E7.

$$E1 = 2.8561 \times \tanh[(Bn \times 0.53035) + (Sn \times 0.49116) - (Wn \times 0.40621) - (FAn \times 2.3467) + (Dn \times 2.1055) + (ATn \times 0.87196) - 2.4344] \quad (2)$$

$$E2 = 1.4268 \times \tanh[(Bn \times 2.56652) + (Sn \times 5.6652) - (Wn \times 1.0366) + (FAn \times 2.4696) - (Dn \times 2.2601) + (ATn \times 1.5209) + 0.15534] \quad (3)$$

$$E3 = -2.1366 \times \tanh[(Bn \times 1.3085) + (Sn \times 0.35256) - (Wn \times 1.1101) + (FAn \times 0.50655) + (Dn \times 0.75319) - (ATn \times 0.17218) - 0.0027526] \quad (4)$$

$$E4 = 0.84238 \times \tanh[(Bn \times 2.9477) - (Sn \times 2.2667) + (Wn \times 0.34965) + (FAn \times 0.97791) - (Dn \times 0.011495) + (ATn \times 0.66825) - 0.077919] \quad (5)$$

$$E5 = 2.4435 \times \tanh[(Bn \times 0.40747) + (Sn \times 0.58673) - (Wn \times 1.0959) + (FAn \times 2.6042) - (Dn \times 1.3285) - (ATn \times 1.1623) + 2.2803] \quad (6)$$

$$E6 = -1.7148 \times \tanh[(Bn \times 0.31346) + (Sn \times 3.4977) + (Wn \times 1.3966) - (FAn \times 0.71556) - (Dn \times 1.1189) - (ATn \times 1.4739) - 2.6024] \quad (7)$$

$$E7 = -1.2093 \times \tanh[-(Bn \times 2.6287) - (Sn \times 0.31735) + (Wn \times 0.13484) + (FAn \times 1.0637) - (Dn \times 2.0254) - (ATn \times 1.2057) - 2.589] \quad (8)$$

$$CSn = \tanh[(E1 + E2 + E3 + E4 + E5 + E6 + E7) - 1.7211] \quad (9)$$

where,

Bn – Normalized binder content (kg/m^3).

Sn – Normalized fine aggregate content or normalized sand content (kg/m^3).

Wn – Normalized water content (kg/m^3).

FAn – Normalized foaming agent content (kg/m^3).

Dn – Normalized density content of FC (kg/m^3).

ATn – Normalized testing age of specimen (days).

CSn – Normalized compressive strength of FC (MPa).

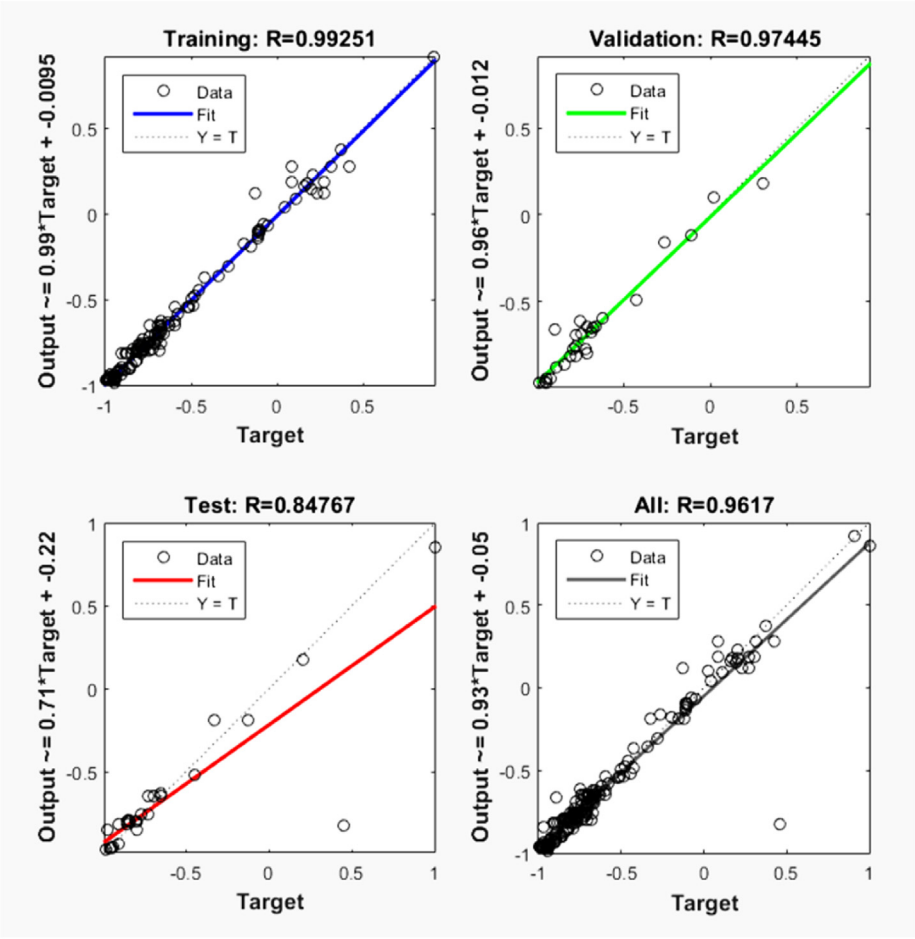

Fig. 19 – Performance of ANN model ($k = 1$) to predict compressive strength.

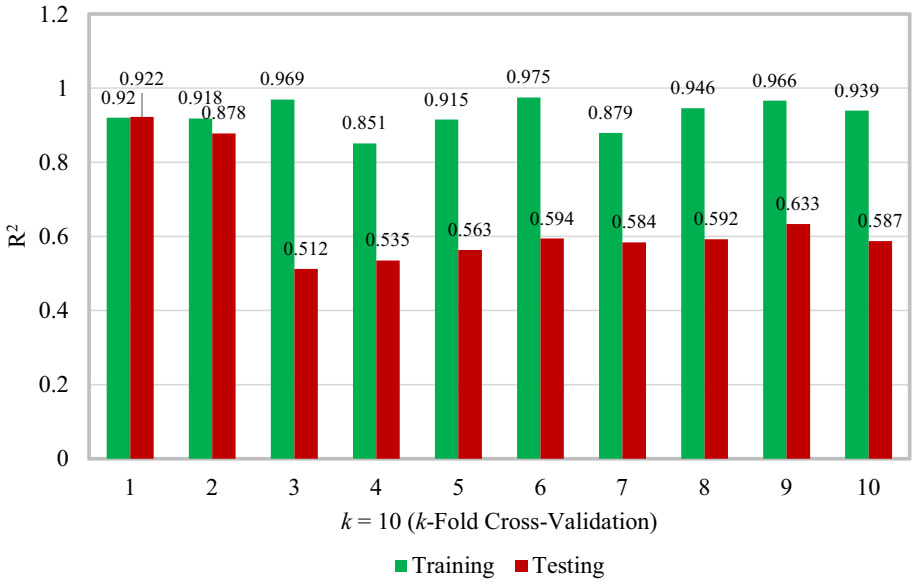

Fig. 20 – k-fold ($k = 1$) cross-validation method for ANN model.

6. Conclusions

The utilization of nanoparticles in FC is currently in the exploratory phase, and the implementation of these particles in construction applications is limited at present. It is certainly probable that nanoparticles have the potential to enhance the physical, mechanical, and durability properties of FC. This study aimed to examine the potential application of different weight fractions (ranging from 1% to 6%) of CCNPs in FC for improving the physical and mechanical properties. The current study yields the following conclusions.

- The increase in the weight percentage of CCNPs decreased the slump flow of FC. The workability of FC was adversely affected by the noticeable specific surface area of CCNPs.
- The inclusion of CCNPs in FC improved the compressive, tensile, and flexural strengths. The recommended weight fraction of CCNPs to be incorporated into FC was 4%. The use of CCNPs enhanced the strength characteristics of FC by promoting the formation of a more compact structure of hydration products. This resulted in the improved particle volume distribution and a reduction in the pore size and interconnectivity.
- The inclusion of more than 4% CCNPs in FC led to the particle clumping and agglomeration, which were caused by the non-uniform dispersion. This ultimately resulted in a reduction in the mechanical properties.
- The increase in the CCNPs weight fraction improved the porosity of FC as well as reduced its capacity to absorb water. The high reactivity of the material decreased the water absorption and permeable porosity. This was achieved by increasing the density of the interfacial transition zone.
- Development of correlation of the mechanical properties of FC-CCNP composites was proposed in this study.
- The compressive strength (output variable) was estimated from seven ingredients (input variables) of FC, using k-fold cross-validation ($k = 1$) with the best R^2 value of 0.921.
- The incorporation of CCNPs into FC led to an increase in the density, thus improving the mechanical and durability properties. This observation was supported by the examination of the morphological characteristics.

Funding

The research was funded by the Ministry of Higher Education (MoHE) of Malaysia under the Fundamental Research Grant Scheme (FRGS) (FRGS/1/2022/TK01/USM/02/3).

Declaration of competing interest

The authors declare that they have no known competing financial interests or personal relationships that could have appeared to influence the work reported in this article.

REFERENCES

[1] Monteiro H, Moura B, Soares N. Advancements in nano-enabled cement and concrete: innovative properties and environmental implications. J Build Eng 2022;56:104736.
[2] Nawi MNM, Lee A, Mydin MAO, Osman WN, Rofie MK. Supply chain management (SCM): disintegration team factors in Malaysian Industrialised Building System (IBS) construction projects. Int J Supply Chain Manag 2018;7(1):140–3.
[3] Mydin MAO, Phius AF, Sani NM, Tawil NM. Potential of green construction in Malaysia: industrialised building system (IBS) vs traditional construction method. E3S Web Conf. 2014;3:01009.
[4] Gemi L, Alsdudi M, Aksoylu C, Yazman Ş, Özkılıç YO, Arslan MH. Optimum amount of CFRP for strengthening shear deficient reinforced concrete beams. Steel Compos Struct 2022;43:735–57.
[5] Özkılıç YO, Aksoylu C, Arslan MH. Numerical evaluation of effects of shear span, stirrup spacing and angle of stirrup on reinforced concrete beam behaviour. Struct Eng Mech 2021;79(3):309–26.
[6] Başaran B, Aksoylu C, Özkılıç YO, Karalar M, Hakamy A. Shear behaviour of reinforced concrete beams utilizing waste marble powder. Structures 2023;54:1090–100.
[7] Özkılıç YO, Başaran B, Aksoylu C, Karalar M, Martins CH. Mechanical behavior in terms of shear and bending performance of reinforced concrete beam using waste fire clay as replacement of aggregate. Case Stud Constr Mater 2023;18:e02104.
[8] Yıldızel SA, Özkılıç YO, Bahrami A, Aksoylu C, Başaran B, Hakamy A, et al. Experimental investigation and analytical prediction of flexural behaviour of reinforced concrete beams with steel fibres extracted from waste tyres. Case Stud Constr Mater 2023:e02227.
[9] Ganesan S, Othuman Mydin MA, Sani NM, Che Ani AI. Performance of polymer modified mortar with different dosage of polymeric modifier. MATEC Web Conf 2014;15:01039.
[10] Mohamad N, Iman MA, Othuman Mydin MA, Samad AAA, Rosli JA, Noorwirdawati A. Mechanical properties and flexure behaviour of lightweight foamed concrete incorporating coir fibre. IOP Conf Ser Earth Environ Sci 2018;140:012140.
[11] Huang H, Li M, Yuan Y, Bai H. Theoretical analysis on the lateral drift of precast concrete frame with replaceable artificial controllable plastic hinges. J Build Eng 2022;62:105386. https://doi.org/10.1016/j.jobe.2022.105386.
[12] Mohamad N, Samad AAA, Lakhiar MT, Othuman Mydin MA, Jusoh S, Sofia A, et al. Effects of incorporating banana skin powder (BSP) and palm oil fuel ash (POFA) on mechanical properties of lightweight foamed concrete. Int J Int Eng 2018;10:169–76.
[13] Serri E, Suleiman MZ, Mydin MAO. The effects of oil palm shell aggregate shape on the thermal properties and density of concrete. Adv Mater Res 2014;935:172–5.
[14] Zhang W, Liu X, Huang Y, Tong M. Reliability-based analysis of the flexural strength of concrete beams reinforced with hybrid BFRP and steel rebars. Arch Civ Mech Eng 2022;22(4):171. https://doi.org/10.1007/s43452-022-00493-7.
[15] Huang H, Yuan Y, Zhang W, Li M. Seismic behavior of a replaceable artificial controllable plastic hinge for precast concrete beam-column joint. Eng Struct 2021;245:112848. https://doi.org/10.1016/j.engstruct.2021.112848S.
[16] Sun L, Wang C, Zhang C, Yang Z, Li C, Qiao P. Experimental investigation on the bond performance of sea sand coral concrete with FRP bar reinforcement for marine

environments. Adv Struct Eng 2022;26(3):533–46. https://doi.org/10.1177/13694332221131153.
[17] Chang Q, Liu L, Farooqi MU, Thomas B, Özkılıç YO. Data-driven based estimation of waste-derived ceramic concrete from experimental results with its environmental assessment. J Mater Res Technol 2023;24:6348–68.
[18] Özkılıç YO, Karalar M, Aksoylu C, Beskopylny AN, Stel'makh SA, Shcherban EM, Azevedo AR. Shear performance of reinforced expansive concrete beams utilizing aluminium waste. J Mater Res Technol 2023;24:5433–48.
[19] Wang M, Yang X, Wang W. Establishing a 3D aggregates database from X-ray CT scans of bulk concrete. Construct Build Mater 2022;315:125740. https://doi.org/10.1016/j.conbuildmat.2021.125740S.
[20] Zhang W, Kang S, Liu X, Lin B, Huang Y. Experimental study of a composite beam externally bonded with a carbon fiber-reinforced plastic plate. J Build Eng 2023;71:106522. https://doi.org/10.1016/j.jobe.2023.106522S.
[21] Fang B, Hu Z, Shi T, Liu Y, Wang X, Yang D, Zhao Z. Research progress on the properties and applications of magnesium phosphate cement. Ceram Int 2022. https://doi.org/10.1016/j.ceramint.2022.11.078.
[22] Tao Shi YLZH. Deformation performance and fracture toughness of carbon nanofiber modified cement-based materials. ACI Mater J 2022;119(5). https://doi.org/10.14359/51735976.
[23] Shi T, Liu Y, Zhao X, Wang J, Zhao Z, Corr DJ, et al. Study on mechanical properties of the interfacial transition zone in carbon nanofiber-reinforced cement mortar based on the PeakForce tapping mode of atomic force microscope. J Build Eng 2022;61:105248. https://doi.org/10.1016/j.jobe.2022.105248.
[24] Tu H, Wei Z, Bahrami A, Kahla NB, Ahmad A, Özkılıç YO. Recent advancements and future trends in 3D printing concrete using waste materials. Developments in the Built Environ 2023:100187.
[25] Zhou S, Lu C, Zhu X, Li F. Preparation and characterization of high-strength geopolymer based on BH-1 lunar soil simulant with low alkali content. Eng 2021;7(11):1631–45. https://doi.org/10.1016/j.eng.2020.10.016.
[26] Rudnai G. Lightweight concretes. Budapest, Hungary: Akademikiado; 1963.
[27] Liu Y, Wang L, Cao K, Sun L. Review on the durability of polypropylene fibre-reinforced concrete. Adv Civ Eng 2021:6652077.
[28] Pakravan HR, Latifi M, Jamshidi M. Hybrid short fiber reinforcement system in concrete: a Review. Construct Build Mater 2017;142:280–94.
[29] Tambichik MA, Abdul Samad AA, Mohamad N, Mohd Ali AZ, Othuman Mydin MA, Mohd Bosro MZ, et al. Effect of combining palm oil fuel ash (POFA) and rice husk ash (RHA) as partial cement replacement to the compressive strength of concrete. Int. J. Integr. Eng. 2018;10:61–7.
[30] Awang H, Mydin MAO, Roslan AF. Effects of fibre on drying shrinkage, compressive and flexural strength of lightweight foamed concrete. Adv Mater Res 2012;587:144–9.
[31] Mydin MAO, Soleimanzadeh S. Effect of polypropylene fiber content on flexural strength of lightweight foamed concrete at ambient and elevated temperatures. Adv Appl Sci Res 2012;3:2837–46.
[32] Ahmed HK, Abbas WA, AlSaff D. Effect of plastic fibers on properties of foamed concrete. Eng Technol J 2013;31:1313–30.
[33] Castillo-Lara JF, Flores-Johnson EA, Valadez-Gonzalez A, Herrera-Franco PJ, Carrillo JG, Gonzalez-Chi PI, et al. Mechanical properties of natural fiber reinforced foamed concrete. Materials 2020;13:3060.
[34] Falliano D, de Domenico D, Ricciardi G, Gugliandolo E. Compressive and flexural strength of fiber-reinforced foamed concrete: effect of fiber content, curing conditions and dry density. Construct Build Mater 2019;198:479–93.
[35] Othuman Mydin MA, Mohd Zamzani N. Coconut fiber strengthen high performance concrete: young's modulus, ultrasonic pulse velocity and ductility properties. Int J Eng Technol 2018;7(2):284–7.
[36] Nensok MH, Mydin MAO, Awang H. Investigation of thermal, mechanical and transport properties of ultra lightweight foamed concrete (UFC) strengthened with alkali treated banana fibre. J Adv Res Fluid Mech Therm Sci 2021;86(1):123–39.
[37] Brostow W, Hagg Lobland HE. Materials: introduction and applications. John Wiley & Sons; 2017.
[38] Song N, Li Z, Yi W, Wang S. Properties of foam concrete with hydrophobic starch nanoparticles as foam stabilizer. J Build Eng 2022;56:104811.
[39] Serri E, Othuman Mydin MA, Suleiman MZ. The influence of mix design on mechanical properties of oil palm shell lightweight concrete. J Mater Environ Sci 2015;6(3):607–12.
[40] Suhaili SS, Mydin MAO, Awang H. Influence of mesocarp fibre inclusion on thermal properties of foamed concrete. J Adv Res Fluid Mech Therm Sci 2021;87(1):1–11.
[41] Gajanan K, Tijare S. Applications of nanomaterials. Mater Today Proc 2018;5:1093–6.
[42] Madenci E, Özkılıç YO, Aksoylu C, Asyraf MRM, Syamsir A, Supian ABM, et al. Experimental and analytical investigation of flexural behavior of carbon nanotube reinforced textile based composites. Materials 2023;16(6):2222.
[43] Madenci E, Özkılıç YO, Aksoylu C, Asyraf MRM, Syamsir A, Supian ABM, et al. Buckling analysis of CNT-reinforced polymer composite beam using experimental and analytical methods. Materials 2023;16(2):614.
[44] Madenci E, Özkılıç YO, Hakamy A, Tounsi A. Experimental tensile test and micro-mechanic investigation on carbon nanotube reinforced carbon fiber composite beams. Adv Nano Res 2023;14(5). https://doi.org/10.12989/anr.2023.14.5.443.
[45] Alhassan M, Alkhawaldeh A, Betoush N, Alkhawaldeh M, Huseien GF, Amaireh L, et al. Life cycle assessment of the sustainability of alkali-activated binders. Biomimetics 2023;8(1):58.
[46] Mydin MAO, Nawi MNM, Omar R, Mohamed Amine K, Ali IM, Deraman R. The use of inorganic ferrous–ferric oxide nanoparticles to improve fresh and durability properties of foamed concrete. Chemosphere 2023;317:137661.
[47] He X, Shi X. Chloride permeability and microstructure of portland cement mortars incorporating nanomaterials. Transp Res Rec J Transp Res Board 2008;2070:13–21.
[48] Chang TP, Shih JY, Yang KM, Hsiao TC. Material properties of portland cement paste with nano-montmorillonite. J Mater Sci 2007;42:7478–87.
[49] Dhiman NK, Sidhu N, Agnihotri S, Mukherjee A, Reddy MS. Role of nanomaterials in protecting building materials from degradation and deterioration. Biodegrad. Biodeterior. Nanoscale 2022:405–75.
[50] Irshidat MR, Al-Saleh MH. Thermal performance and fire resistance of nanoclay modified cementitious materials. Construct Build Mater 2018;159:213–9.
[51] Nehdi ML. Clay in cement-based materials: critical overview of state-of-the-art. Construct Build Mater 2014;51:372–82.
[52] Hou L, Li J, Lu Z, Niu Y, Jiang J, Li T. Effect of nanoparticles on foaming agent and the foamed concrete. Construct Build Mater 2019;227:116698.
[53] Huang Z, Zhang T, Wen Z. Proportioning and characterization of Portland cement-based ultra-

lightweight foam concretes. Construct Build Mater 2015;79:390–6.
[54] Du HJ, Du SH, Liu XM. Durability performances of concrete with nano-silica. Construct Build Mater 2014;73:705–12.
[55] Rong Z, Sun W, Xiao H, Jiang G. Effects of nano-SiO_2 particles on the mechanical and microstructural properties of ultra-high performance cementitious composites. Cem Concr Compos 2015;56:25–31.
[56] Norhasri MM, Hamidah M, Fadzil AM. Applications of using nano material in concrete: a review. Construct Build Mater 2017;133:91–7.
[57] Gokçe HS, Hatungimana D, Ramyar K. Effect of fly ash and silica fume on hardened properties of foamed concrete. Construct Build Mater 2019;194:1–11.
[58] Zhang YQ, Chang ZD, Luo WL, Gu SN, Li WJ, An JB. An effect of starch particles on foam stability and dilational viscoelasticity of aqueous-foam. Chin J Chem Eng 2015;23:276–80.
[59] Liu X, Chen L, Liu A, Wang X. Effect of nano-$CaCO_3$ on properties of cement paste. Energy Proc 2012;16:991–6.
[60] Seifan M, Mendoza S, Berenjian A. Mechanical properties and durability performance of fly ash based mortar containing nano and micro-silica additives. Construct Build Mater 2020;252:119121.
[61] Othuman Mydin MA, Mohd Nawi MN, Mohamed O, Sari MW. Mechanical properties of lightweight foamed concrete modified with magnetite (Fe_3O_4) nanoparticles. Materials 2022;15(17):5911.
[62] Adak D, Sarkar M, Mandal S. Effect of nano-silica on strength and durability of fly ash based geopolymer mortar. Construct Build Mater 2014;70:453–9.
[63] Poudyal L. Use of nanotechnology in concrete. Lubbock, TX, USA: Texas Tech University; 2018.
[64] Shah SP, Hou P, Konsta-Gdoutos MS. Nano-modification of cementitious material: toward a stronger and durable concrete. J Sustain Cem Mater 2015;5:1–22.
[65] Batuecas E, Liendo F, Tommasi T, Bensaid S, Deorsola F, Fino D. Recycling CO_2 from flue gas for $CaCO_3$ nanoparticles production as cement filler: a Life Cycle Assessment. J CO2 Util 2021;45:101446.
[66] Poudyal L, Adhikari K, Won M. Mechanical and durability properties of portland limestone cement (PLC) incorporated with nano calcium carbonate ($CaCO_3$). Materials 2021;14:905.
[67] Poudyal L, Adhikari K. Environmental sustainability in cement industry: an integrated approach for green and economical cement production. Resour Environ Sustain 2021;4:100024.
[68] BS EN 197-1. Cement - composition, specifications and conformity criteria for common cements. London, UK: British Standards Institute; 2011.
[69] ASTM C33-03. Standard specification for concrete aggregates. American society for testing and materials. West Conshohocken, PA: ASTM International; 2003.
[70] ASTM C128-15. Standard test method for relative density (specific gravity) and absorption of fine aggregate. American society for testing and materials. West Conshohocken, PA: ASTM International; 2015.
[71] BS EN 3148. Water for making concrete (including notes on the suitability of the water). London, UK: British Standards Institute; 1980.
[72] Mydin MAO, Nawi MNM, Munaaim MAC, Mohamad N, Samad AAA, Johari I. Effect of steel fibre volume fraction on thermal performance of Lightweight Foamed Mortar (LFM) at ambient temperature. J Adv Res Fluid Mech Therm Sci 2018;47(1):119–26.
[73] ASTM C1437-20. Standard test method for flow of hydraulic cement mortar. American society for testing and materials. West Conshohocken, PA: ASTM International; 2020.
[74] BS EN 12390-5. Testing hardened concrete. Flexural strength of test specimens. London, UK: British Standards Institute; 2019.
[75] BS EN 12390-3. Testing hardened concrete. Compressive strength of test specimens. London, UK: British Standards Institute; 2011.
[76] BS EN 12390-6. Testing hardened concrete. Tensile splitting strength of test specimens. London, UK: British Standards Institute; 2009.
[77] Amran Y, Farzadnia N, Abang Ali A. Properties and applications of foamed concrete; a review. Construct Build Mater 2015;101:990–1005.
[78] BS EN 1881-122. Testing concrete Method for determination of water absorption. London, UK: British Standards Institute; 2020.
[79] ASTM C878/C878M-22. Standard test method for restrained expansion of shrinkage-compensating concrete. American society for testing and materials. West Conshohocken, PA: ASTM International; 2022.
[80] ASTM C 230-97. Flow table for use in tests of hydraulic cement. American society for testing and materials. West Conshohocken, PA: ASTM International; 1997.
[81] Supit SWM, Shaikh FUA. Durability properties of high volume fly ash concrete containing nano-silica. Mater Struct 2015;48(8):2431–45.
[82] Meng T, Qian KL, Qian XQ. Effect of composite nano-addition on mechanics strength and microstructure of cement paste. Rare Met Mater Eng 2008;37:631–3.
[83] Othuman Mydin MA. Evaluation of the mechanical properties of lightweight foamed concrete at varying elevated temperatures. Fire 2023;6(2):53.
[84] Nensok MH, Mydin MAO, Awang H. Fresh state and mechanical properties of ultra-lightweight foamed concrete incorporating alkali treated banana fibre. J Teknol 2022;84(1):117–28.
[85] Musa M, Othuman Mydin MA, Abdul Ghani AN. Influence of oil palm empty fruit bunch (EFB) fibre on drying shrinkage in restrained lightweight foamed mortar. Int J Innovative Technol Explor Eng 2019;8(10):4533–8.
[86] Ganesan S, Othuman Mydin MA, Mohd Yunos MY, Mohd Nawi MN. Thermal properties of foamed concrete with various densities and additives at ambient temperature. Appl Mech Mater 2015;747:230–3.
[87] Nazari A, Riahi S, Shirin R, Seyedeh FS, Khademno A. The effects of incorporation Fe2O3 nano particles on tensile and flexural strength of concrete. J Am Sci 2010;6:90–3.
[88] Hakamy A. Effect of $CaCO_3$ nanoparticles on the microstructure and fracture toughness of ceramic nanocomposites. J Taibah Univ Sci 2020;14(1):1201–7.
[89] Liu X, Wang X, Liu A. Study on the mechanical properties of cement modified by nanoparticles. Appl Mech Mater 2012;157–158:161–4.
[90] Shaikh FU, Supit SWM. Mechanical and durability properties of high volume fly ash concrete containing calcium carbonate nanoparticles. Construct Build Mater 2014;70:309–21.
[91] Mansi A, Sor NH, Hilal N, Qaidi SMA. The impact of nano clay on normal and high-performance concrete characteristics: a review. IOP Conf Ser Earth Environ Sci 2022;961:012085.
[92] Han B, Li Z, Zhang L, Zeng S, Yu X, Han B, et al. Reactive powder concrete reinforced with nano SiO_2-coated TiO_2. Construct Build Mater 2017;148:104–12.
[93] Mohammed A, Rafiq S, Mahmood W, Al-Darkazalir H, Noaman R, Qadir W, et al. Artificial Neural Network and NLR techniques to predict the rheological properties and compression strength of cement past modified with nanoclay. Ain Shams Eng J 2021;12:1313–28.

[94] Nejad FM, Tolouei M, Nazari H, Naderan A. Effects of calcium carbonate nanoparticles and fly ash on mechanical and permeability properties of concrete. Adv Civ Eng Mater 2018;7(1):651–68.
[95] Emamian SA, Eskandari-Naddaf H. Effect of porosity on predicting compressive and flexural strength of cement mortar containing micro and nano-silica by ANN and GEP. Construct Build Mater 2019;218:8–27.
[96] Martinez-Garcia R, Sanchez de Rojas MI, Jagadesh P, Lopez-Gayarre F, Moran-del-Pozo JM, Juan-Valdes A. Effects of pores on the mechanical and durability properties on high strength recycled fine aggregate mortar. Case Stud Constr Mater 2022;16:e01050.
[97] Roslan AF, Awang H, Mydin MAO. Effects of various additives on drying shrinkage, compressive and flexural strength of lightweight foamed concrete. Adv Mater Res 2013;626:594–604.
[98] Abellan-Garcia J, Iqbal Khan M, Abbas YM, Martínez-Lirón V, Carvajal-Muñoz JS. The drying shrinkage response of recycled-waste-glass-powder-and calcium-carbonate-based ultrahigh-performance concrete. Construct Build Mater 2023:131163.
[99] Ni K, Shi Y, Hu Z, Zhang Y, Wan P. Effect of coal gangue grain size on strength of foam concrete. J Phys Conf 2020;1635:012080.
[100] Xiao J, Zhang H, Zou S, Duan Z, Ma Y. Developing recycled foamed concrete for engineered material arresting system. J Build Eng 2022;53:104555.
[101] Serudin AM, Mydin MAO, Ghani ANA. Influence of fibreglass mesh on physical properties of lightweight foamcrete. IIUM Engineering Journal 2021;22(1):23–34.
[102] Jagadesh P, Nagarajan V, Karthik Prabhu T, Karthik Arunachalam K. Effect of nano titanium di oxide on mechanical properties of fly ash ad ground granulated blast furance slage based geopolymer concrete. J Build Eng 2022;61:105235.
[103] Ramezanianpour AA, Ghiasvand E, Nickseresht L, Mahdikhani M, Moodi F. Influence of various amounts of limestone powder on the performance of Portland limestone cement concretes. Cement Concr Compos 2009;31:715–20.
[104] Martinez-Garcia R, Jagadesh P, Burdalo-Salcedo G, Palencia C, Fernandez-Raga M, Fraile-Fernandez FJ. Impact of design parameters on the ratio of compressive to spilt tensile strength of self-compacting concrete with recycled aggregate. Materials 2021;14(13):3480.
[105] Isleem HF, Jagadesh P, Ahmad J, Qaidi SMA, Althoey F, Najm HM, et al. Finite element and analytical modelling of PVC-confined concrete columns under axial compression. Front Mater 2022;9:1011675.
[106] Tikalsky PJ, Pospisil J, MacDonald W. A method for assessment of the freeze–thaw resistance of preformed foam cellular concrete. Cement Concr Res 2004;34(5):889–93.